

Electronic structure of thioether containing NSNO donor azo-ligand and its copper(II) complex: Experimental and theoretical studies



Ajoy Kumar Pramanik, Deblina Sarkar, Tapan Kumar Mondal*

Inorganic Chemistry Section, Department of Chemistry, Jadavpur University, Kolkata 700032, India

ARTICLE INFO

Article history:

Received 21 March 2015

Received in revised form

8 June 2015

Accepted 13 June 2015

Available online 19 June 2015

ABSTRACT

Synthesis of thioether containing NSNO donor azo ligand (HL) showing hydrazoketo and azoenol tautomerism has been performed. The hydrazoketo and azoenol equilibrium of HL has been studied. The hydrazoketo form of HL is predominating over azoenol form. In copper(II) complex the ligand is present in azoenol form. The electronic spectra and electronic structure of the complex has been extensively studied. The structures of the ligand and copper(II) complex have been established from single crystal X-ray studies. The 1-D supramolecular structure of the complex is formed by $\pi-\pi$ interactions.

© 2015 Elsevier B.V. All rights reserved.

Keywords:

Hydrazoketo and azoenol tautomerism

NSNO donor azo ligand

X-ray and electronic structure

DFT and TDDFT calculations

1. Introduction

Azo compounds are a very important class of chemical compounds receiving attention in scientific research for the last few decades. They are highly colored and have been used as dyes and pigments for a long time [1,2]. Furthermore, they have been studied widely because of their excellent thermal and optical properties in applications such as optical recording medium [3], toner [4,5] and ink-jet printing [6,7]. Recently, azo metal chelates have also attracted increasing attention due to their interesting electronic and geometrical features in connection with their application for molecular memory storage, nonlinear optical elements, and printing systems [8].

In this work we have synthesized thioether containing NSNO donor azo ligand (HL) showing hydrazoketo and azoenol tautomerism (Scheme 1). The equilibrium between the hydrazoketo and azoenol forms of organic molecules, containing the $\text{HN}-\text{N}=\text{C}-\text{C}=\text{O}$ group, is well known. This process has been studied because of their importance in the dyestuff industry and as acid–base indicators [9]. The organic compounds containing this group show strong intramolecular hydrogen bonding between the N–H and CO fragments [10–12]. Strong hydrogen bonds occur due to the fact that the neutral donor and acceptor atoms are connected by a

system of π -conjugated double bonds; this system has been referred to as RAHB (resonance-assisted hydrogen bonding). It has been used successfully to explain intra- and inter-molecular O–H ... O hydrogen bonds in compounds containing the β -diketo enol fragment [13–16] and to explain N–H ... O bonds in molecules containing the $\text{HN}-\text{N}=\text{C}-\text{C}=\text{O}$ fragment [17–19]. The X-ray structure of $[\text{H}_2\text{L}](\text{ClO}_4)$ reveals the existence of hydrazoketo form in the solid state which is further supported by spectral studies. When HL binds with Cu^{2+} the equilibrium is shifted from hydrazoketo to azoenol form and is supported by the X-ray structure of $[\text{Cu}(\text{L})(\text{H}_2\text{O})](\text{ClO}_4)$. The hydrazoketo to azoenol tautomerism of HL and the electronic structure of Cu(II) complex have been interpreted by DFT studies.

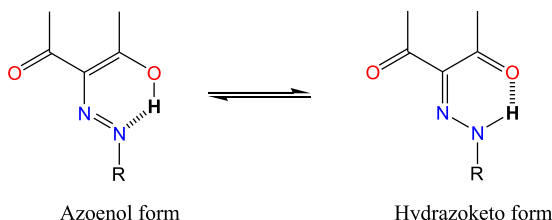
2. Experimental

2.1. Materials

All the reagents and solvents were purchased from commercial sources and used as received. 2-Aminothiophenol and 2-(chloromethyl)pyridine hydrochloride was purchased from Sigma Aldrich. 2-((Pyridine-2-yl)methylthio)benzenamine was prepared following the published procedure [20]. Acetyl acetone (acac) and inorganic metal salts were made available from E. Merck, India. All other organic chemicals and inorganic salts used were of A.R. quality and were available from Sisco Research Lab, Mumbai, India and did not require further purification. The solutions spectral

* Corresponding author.

E-mail address: tkmondal@chemistry.jdvu.ac.in (T.K. Mondal).

**Scheme 1.** Hydrazoketo and azoenol equilibrium of HL.

studies were carried out using spectroscopic grade solvents from Lancaster, U.K. Commercially available SRL silica gel (60–120 mesh) was used for column chromatography.

Caution! Perchlorate salts of transition metal complexes containing organic ligands are potentially explosive [21]! Only small quantities of material should be prepared, and they should be handled with great caution.

2.2. Physical measurements

Melting Point of the ligand was determined using a digital melting point apparatus. Microanalyses (C, H, N) were performed using a Perkin–Elmer Series-II CHN-2400 CHNS/O elemental analyzer. The electronic spectra were measured on Lambda 750 Perkin Elmer spectrophotometer in acetonitrile solution. The IR spectra were recorded on RX-1 Perkin Elmer spectrometer in the spectral range 4000–400 cm⁻¹ with the samples in the form of KBr pellets. ¹H NMR spectrum of HL was recorded in CDCl₃ on Bruker (AC) 300 MHz FT-NMR spectrometer in presence of TMS as internal standard. ESI mass spectra were recorded on a micro mass Q-TOF mass spectrometer. Molar conductance was measured using Systronics conductivity meter (Model 304) using 10⁻³ M solution in acetonitrile.

2.2.1. Synthesis of ligand (HL)

2-((Pyridine-2-yl)methylthio)benzenamine (1.729 g, 8.0 mmol) was dissolved in 10 ml 12(N) HCl. Then it was cooled in ice and an ice cold NaNO₂ (0.552 g, 8.0 mmol) solution was added to this ice cold amine solution dropwise at 0–5 °C under stirring condition and the resulting solution was kept in an ice-bath. Separately, an ice cold solution of acetylacetone (0.801 g, 8 mmol) was prepared in 5(N) Na₂CO₃ (6.36 g in 50 ml water) solution. The diazotized solution was then slowly added to the cold alkaline solution with vigorous stirring. Stirring was continued for 30 min after the addition was complete. The whole mixture was then kept under refrigeration for 1 h. Yellow precipitate of HL was obtained. The crude product was collected by filtration, washed thoroughly with water and dissolved in minimum volume of 1(N) HCl and then Na₂CO₃ solution was added to it for reprecipitation of the compound. It was then filtered again and washed with distilled water. Finally dried over CaCl₂. The dry mass was dissolved in minimum volume of CH₂Cl₂ and was purified by column chromatographic separation on silica gel. An orange-yellow band was eluted with EA-PE (1:3, v/v).

[HL]: Orange-yellow solid, Yield was 1.758 g, (62%); Decomposition temperature ~ 67 °C. Anal. Calc. for C₁₇H₁₇N₃O₂S: C, 62.36; H, 5.23; N, 12.83. Found (%): C, 62.57; H, 5.27; N, 12.91%. IR data (KBr disc) (cm⁻¹): 3430 ν(N–H), 2926 ν(C–H), 1673 ν(C=O), 1577 ν(C=N), 1505 ν(C=C), 1438 ν(N=N). ¹H NMR data in CDCl₃ (δ , ppm): 14.97 (s, 1H), 8.43 (d, J = 5.2 Hz, 1H), 7.74 (d, J = 8.2 Hz, 1H), 7.52 (d, J = 8.5 Hz, 1H), 7.36–7.39 (m, 2H), 7.47 (d, J = 7.8 Hz, 1H), 7.06–7.10 (m, 2H), 4.11 (s, 3H), 2.62 (s, 3H), 2.48 (s, 3H). λ_{Max} (ϵ , M⁻¹ cm⁻¹) in acetonitrile: 403 (sh), 368 (21086), 255 (17210). ESI-MS, m/z : 328



2.2.2. Synthesis of copper(II) complex

To an absolute ethanolic solution (15 ml) of HL (0.327 g, 1.0 mmol), 10 ml ethanolic solution of hydrated metal salt of Cu(ClO₄)₂·6H₂O (0.371 g, 1.0 mmol) was added dropwise under magnetically stirring condition. The stirring was continued gently for six hours. The resultant orange yellow solution changed to dark green during the course of reaction. The reaction mixture was filtered and the resultant solution was kept undisturbed for slow evaporation of the solvent in air. Upon subsequent concentration over a week, two types of crystals were deposited on the wall of beaker. The dark green crystals of complex was separated first, washed with ethanol and hexane and dried over CaCl₂. Then a deep yellow crystalline compound of ligand suitable for single crystal X-ray study was found.

[Cu(L) (H₂O)](ClO₄): Deep green crystalline compound. Yield: 0.237 g (54%); Anal. Calc. for C₁₇H₁₈N₃O₇SCuCl: C, 40.24; H, 3.58; N, 8.28. Found: C, 40.27; H, 3.81; N, 8.92%. IR data (KBr disc) (cm⁻¹): 3450–3436 ν(O–H), 1667 ν(C=O), 1417 ν(N=N), 1082, 1117 ν(ClO₄⁻). λ_{Max} (ϵ , M⁻¹ cm⁻¹) in acetonitrile: 589(452), 527(447), 416(13917), 381(sh), 290(13485), 263(18169). ESI-MS, m/z : 508 [MH]⁺. A_M = 117 Ω⁻¹ mol⁻¹ cm² in acetonitrile.

2.3. Crystal structure determination and refinement

Crystals suitable for X-ray diffraction study of [H₂L](ClO₄) and [Cu(L) (H₂O)](ClO₄) were grown by slow evaporation of the solvent in air kept undisturbed at room temperature and at ambient condition for a week. Complex [Cu(L) (H₂O)](ClO₄) crystallizes contemporarily with HL as [H₂L](ClO₄). Details of crystal analyses, data collection and structure refinement data are given in Table 1. The X-ray data were collected on a Bruker AXS Kappa smart Apex-II diffractometer equipped with an Apex-II CCD area detector using a fine focus sealed tube as the radiation source of graphite monochromator Mo K α radiation (λ = 0.71073 Å). Unit cell parameters were determined from least-squares refinement method. Reflection data were recorded using the ω scan technique. Data were corrected for Lorentz polarization effects and for linear decay. Semi-empirical absorption corrections based on ψ -scans were applied. The structure was solved and refined by full-matrix least-squares techniques on F^2 using WinGX [22] and the SHELXL-97 [23] program. The absorption corrections were done by the multi-scan technique. The data were reduced and integrated using the SAINT [24] program. A Semi-empirical multi-scan absorption correction was made with SADABS [25]. All data were corrected for Lorentz and polarization effects, and the non-hydrogen atoms were refined anisotropically with SHELXS-97 [23]. Hydrogen atoms were generated in the refinement process as per the riding model with thermal parameters equal to 1.2 times that of associated C atoms, and participated in the calculation of the final R-indices. All calculations were carried out using SHELXS 97 [23]. Figures of the structure were drawn with ORTEP-32 [26] programs with 35% ellipsoidal probability.

2.4. Computational details

All computations were performed using the Gaussian09 (G09) program [27]. Full geometry optimizations of ligand and copper complex were carried out using the density functional theory method at the RB3LYP and UB3LYP level of theory [28,29]. The 6-31G(d) basis set for C, H, N, O and S atoms was used. The LanL2DZ basis set with effective core potential was employed for the copper atom [30–32]. The vibrational frequency calculations were performed to ensure that the optimized geometries represent the local

Table 1Summarized crystallographic data and refinement parameters for $[H_2L](ClO_4)$ and $[Cu(L)(H_2O)](ClO_4)$.

| Formula | $C_{17}H_{18}ClN_3O_6S$ | $C_{17}H_{18}ClCuN_3O_7S$ |
|---|-------------------------------|---------------------------------|
| Formula weight | 427.85 | 507.39 |
| Crystal color | Orange yellow | Green |
| Crystal system | Triclinic | Monoclinic |
| Space group | P-1 | P21/c |
| a, b, c [Å] | 5.043(5), 8.234(5), 24.362(5) | 10.6998(4) 13.3428(6) |
| α (°) | 81.297(5) | 14.8222(6) |
| β (°) | 86.093(5) | 90.00 |
| γ (°) | 82.150(5) | 106.302(2) |
| V [Å ³] | 989.4(12) | 2031.02(14) |
| Z | 2 | 4 |
| D(calc) [g/cm ³] | 1.436 | 1.659 |
| $M_u(Mo-K_\alpha)/mm^{-1}$ | 0.338 | 1.356 |
| F(000) | 444 | 1036 |
| Crystal size [mm ³] | 0.22 × 0.18 × 0.15 | 0.23 × 0.17 × 0.15 |
| Data collection | | |
| Absorption correction | Multi-scan | Multi-scan |
| Temperature (K) | 293(2) | 293(2) |
| Radiation [Å] | 0.71073 | 0.71073 |
| θ (Min-Max) [0] | 1.69–25.00 | 1.98–25.50 |
| Dataset (h; k; l) | -5 to 5, -9 to 9, -28 to 28 | -12 to 12; -14 to 16; -17 to 17 |
| Total, unique data, R(int) | 13955, 3449, 0.0537 | 14905, 3727, 0.0434 |
| Observed data [$ I > 2\sigma(I)$] | 2840 | 2944 |
| Refinement | | |
| Nref, Npar | 3371, 301 | 3727, 273 |
| R, wR_2 | 0.0655, 0.1337 | 0.0860, 0.0687 |
| $\Delta\chi(\text{max})$ and $\Delta\chi(\text{min})$ (e/Å ³) | 0.930, 0.951 | 1.689, 1.740 |
| Goodness of fit(S) | 1.016 | 0.994 |

minima of potential energy surface and there are only positive Eigen-values. The lowest 40 singlet–singlet vertical electronic excitations based on B3LYP optimized geometries were computed using the time-dependent density functional theory (TD-DFT) formalism [33–35] in acetonitrile using conductor-like polarizable continuum model (CPCM) [36–38] using the same B3LYP level and basis sets. GaussSum [39] was used to calculate the fractional contributions of various groups to each molecular orbital.

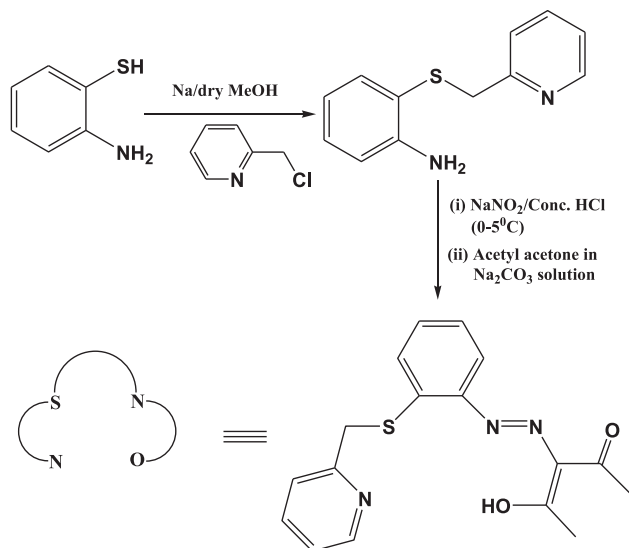
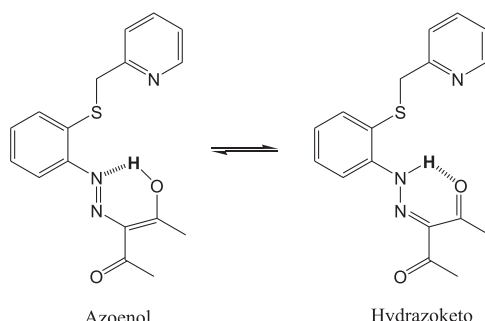
3. Results and discussion

3.1. Synthesis and formulation

A thioether containing tetradentate monobasic NSNO donor ligand (HL) has been synthesized with high yield and in a desirable reaction time (Scheme 2). The ligand is characterized by several spectroscopic techniques and elemental analysis. The 1H NMR signals taken in $CDCl_3$ well supported the proposed structure of the ligand. The S-methylene protons appear at 4.11 ppm as sharp singlet, $-\text{CH}_3$ protons of acetylacetone part appear as sharp singlets at 2.42 and 2.61 ppm. The well resolved aromatic protons appear at 7.06–8.43 ppm. The characteristic hydrogen bonded broad singlet peak corresponds to O–H or N–H appears at 14.97 ppm. IR spectrum of ligand shows characteristic $\nu(X–\text{H})$ ($X = \text{O}$ or N), and $\nu(\text{N}=\text{N})$ at 3430 and 1438 cm⁻¹ respectively. The $\nu(\text{C=O})$ of the ligand appears at 1673 cm⁻¹.

The ligand may exist either in hydrazoketo form or may be in equilibrium (Scheme 3). To study the hydrazoketo and azoenol equilibrium of HL , potential energy scan has been carried out (Fig. 1). The energy scan shows that the hydrazoketo form is more stable by 10.19 kcal/mol compared to the azoenol form of the ligand which supports the experimental results as well. The existence of hydrazoketo form is again supported from the single X-ray crystal structure of HL .

In presence of Cu^{2+} in solution the equilibrium is shifted towards azoenol form and the ligand gets coordinated to copper(II) in azoenol form which is well supported by spectral studies and

**Scheme 2.** Synthetic route of HL .**Scheme 3.** Azoenol and hydrazoketo equilibrium of HL .

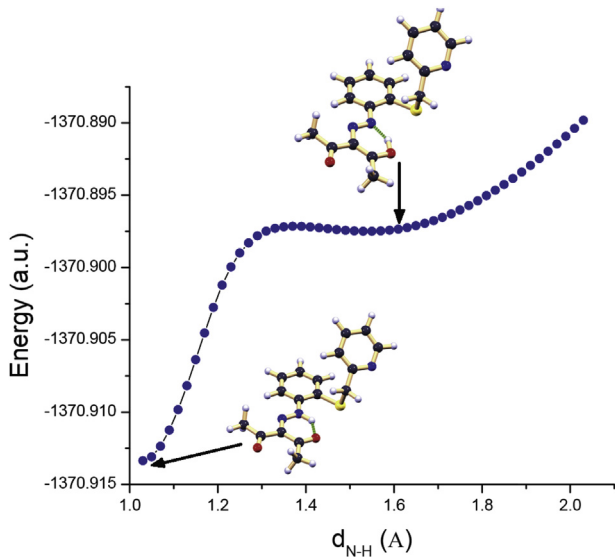
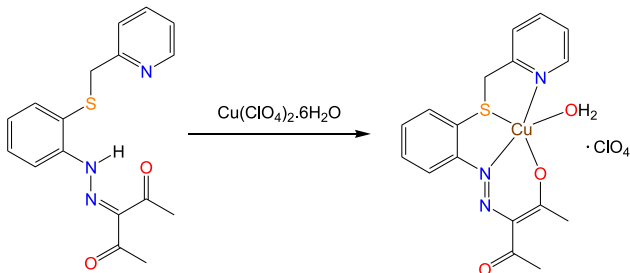


Fig. 1. Potential energy scan with the variation of N–H bond distance by DFT/B3LYP/6-31G(d) method.



Scheme 4. Synthesis of copper(II) complex with HL.

confirmed by single crystal X-ray structure of [Cu(L)(H₂O)](ClO₄). The synthesis of copper(II) complex is shown in Scheme 4. The IR spectrum of the complex shows $\nu(\text{N}=\text{N})$ at 1417 cm⁻¹, $\nu(\text{ClO}_4^-)$ at 1082 and 1117 cm⁻¹ which well supports the complex formation and the splitting of $\nu(\text{ClO}_4^-)$ stretching indicates the H-bonded

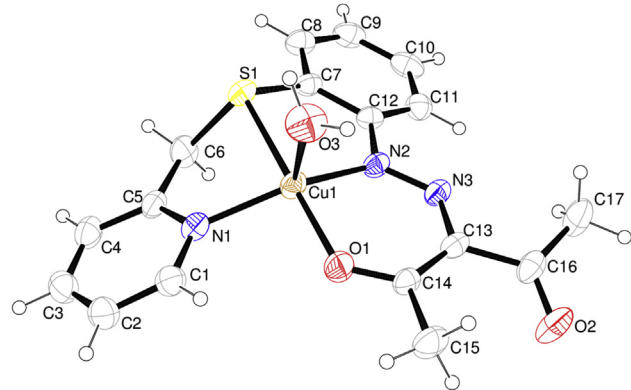


Fig. 3. ORTEP plot of [Cu(L)(H₂O)]⁺ with 35% ellipsoidal probability.

Table 2
Some selected bond distances (Å) and angles (°) of [H₂L](ClO₄).

| Bonds(Å) | X-ray | Angles (°) | X-ray |
|-------------|----------|-------------------|-----------|
| N(2)-N(3) | 1.315(4) | C(6)-S(1)-C(7) | 101.8(2) |
| S(1)-C(6) | 1.828(4) | C(12)-N(2)-N(3) | 120.1(3) |
| N(3)-C(13) | 1.307(4) | O(1)-C(14)-C(13) | 119.3(3) |
| O(1)-C(14) | 1.219(5) | O(1)-C(14)-C(15) | 119.4(3) |
| O(2)-C(16) | 1.209(5) | N(2)-N(3)-C(13) | 121.0(3) |
| C(13)-C(14) | 1.478(5) | N(3)-C(13)-C(14) | 123.9(3) |
| N(3)-C(13) | 1.307(4) | N(3)-C(13)-C(16) | 113.1(3) |
| | | C(13)-C(16)-O(2) | 121.3(3) |
| | | O(2)-C(16)-C(17) | 120.5 (4) |
| | | C(13)-C(16)-C(17) | 118.1(3) |
| | | C(13)-C(14)-C(15) | 121.2(3) |

interaction in the molecule [40]. To know the electrolytic nature of the complex in solution, conductivity measurement has been carried out. The molar conductance (Λ_M) of complex in CH₃CN is 126 Ω⁻¹cm² mol⁻¹. Thus, the complex is 1:1 electrolyte in acetonitrile.

3.2. X-ray structure

The ligand HL and the copper(II) complex crystallize from

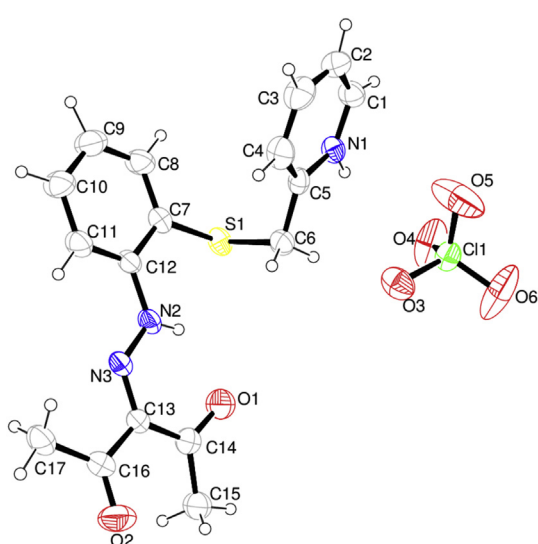


Fig. 2. ORTEP plot of [H₂L](ClO₄) with 35% ellipsoidal probability.

Table 3
Selected bond distances (Å) and bond angles (°) of [Cu(L)(H₂O)](ClO₄).

| Bonds(Å) | X-ray | DFT/B3LYP |
|-----------------|------------|-----------|
| Cu(1)-N(1) | 1.990(5) | 2.096 |
| Cu(1)-N(2) | 1.914(5) | 1.977 |
| Cu(1)-O(1) | 1.915(4) | 1.947 |
| Cu(1)-O(3) | 2.296(5) | 2.282 |
| Cu(1)-S(1) | 2.2730(14) | 2.392 |
| N(2)-N(3) | 1.296(6) | 1.281 |
| N(3)-C(13) | 1.349(7) | 1.335 |
| C(13)-C(16) | 1.486(8) | 1.453 |
| O(1)-C(14) | 1.258(6) | 1.265 |
| O(2)-C(16) | 1.212(7) | 1.220 |
| Angles (°) | | |
| N(1)-Cu(1)-N(2) | 149.59(19) | 143.34 |
| N(2)-Cu(1)-O(1) | 91.48(18) | 90.84 |
| N(1)-Cu(1)-O(3) | 104.40(19) | 97.98 |
| N(1)-Cu(1)-S(1) | 85.36(13) | 83.62 |
| N(1)-Cu(1)-O(1) | 94.88(18) | 97.92 |
| N(2)-Cu(1)-O(3) | 105.73(19) | 118.09 |
| N(2)-Cu(1)-S(1) | 88.44(13) | 86.84 |
| O(1)-Cu(1)-O(3) | 85.5(2) | 86.62 |
| O(1)-Cu(1)-S(1) | 179.66(15) | 177.61 |
| O(3)-Cu(1)-S(1) | 94.21(15) | 94.98 |

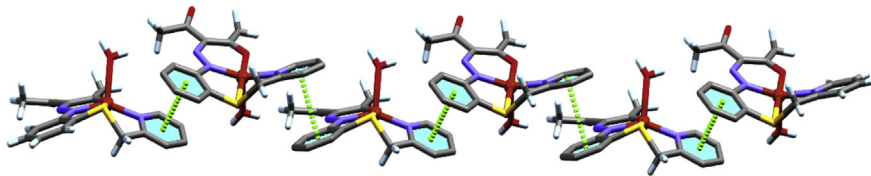


Fig. 4. 1D supramolecular network involving $\pi\cdots\pi$ interaction along c-axis for $[\text{Cu}(\text{L})(\text{H}_2\text{O})]^+$.

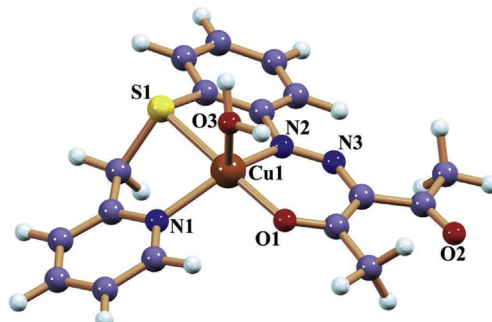


Fig. 5. Optimized structure of $[\text{Cu}(\text{L})(\text{H}_2\text{O})]^+$ by DFT/B3LYP method.

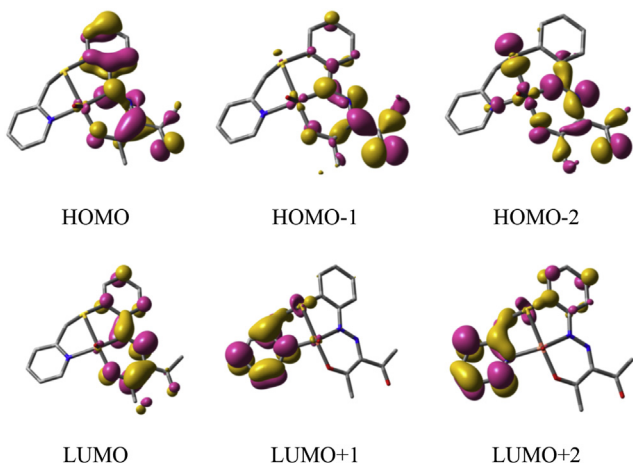


Fig. 6. Contour plots of selected molecular orbitals (α -spin) of $[\text{Cu}(\text{L})(\text{H}_2\text{O})]^+$.

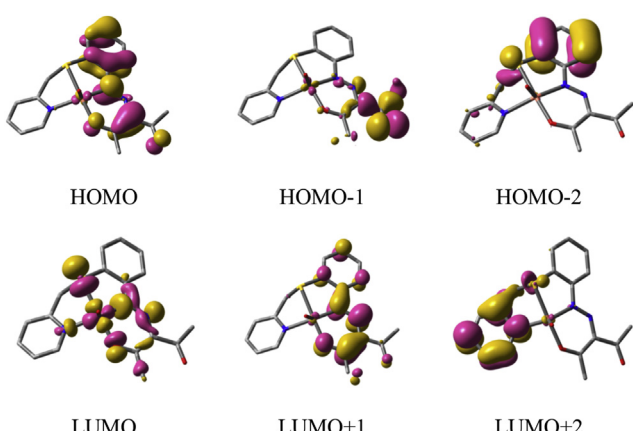


Fig. 7. Contour plots of selected molecular orbitals (β -spin) of $[\text{Cu}(\text{L})(\text{H}_2\text{O})]^+$.

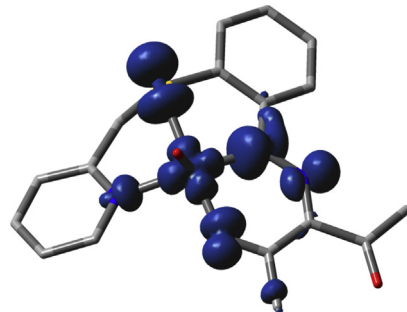


Fig. 8. Spin density plot of $[\text{Cu}(\text{L})(\text{H}_2\text{O})]^+$.

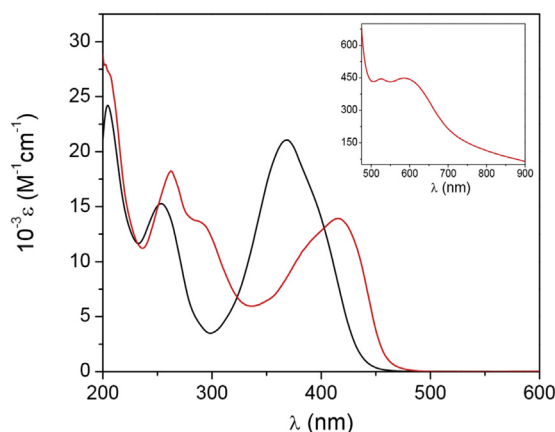
methanol–water mixture. The complex crystallizes with aqua ligand in the metal coordination sphere. Complex $[\text{Cu}(\text{L})(\text{H}_2\text{O})](\text{ClO}_4)$ crystallizes contemporarily with HL as $[\text{H}_2\text{L}](\text{ClO}_4)$. The ORTEP plots of HL and its copper complex are shown in Figs. 2 and 3 respectively. The bond parameters for $[\text{H}_2\text{L}](\text{ClO}_4)$ supports the hydrazoketo form. The $\text{O}(1)\text{-C}(14)$ and $\text{O}(2)\text{-C}(16)$ bond distances are $1.219(5)$ and $1.209(5)$ Å which perfectly match with the C=O bond distances. The hydrazoketo form of the ligand are supported by the shorter $\text{N}(3)\text{-C}(13)$ ($1.307(4)$ Å) and longer $\text{C}(13)\text{-C}(14)$ ($1.478(5)$ Å) bond distances (Table 2). The longer $\text{N}(2)\text{-N}(3)$, $1.315(4)$ Å also confirms the existence of hydrazoketo form of the ligand. In $[\text{Cu}(\text{L})(\text{H}_2\text{O})](\text{ClO}_4)$, copper is penta-coordinated having the geometry intermediate between distorted square pyramid and trigonal bipyramidal. The trigonality index [41] τ value is 0.50 [$\tau = (\beta - \alpha)/60$ where α and β are the main opposed angles in the coordination polyhedron and for perfect square pyramidal and trigonal bipyramidal geometries the values of τ are zero and unity respectively. In the present case $\beta = \text{O}(1)\text{-Cu}(1)\text{-S}(1) = 179.66(15)^\circ$ and $\alpha = \text{N}(1)\text{-Cu}(1)\text{-N}(2) = 149.59(19)^\circ$] (Table 3). According to the

Table 4
Energy and composition of selected molecular orbitals (α -spin) of $[\text{Cu}(\text{L})(\text{H}_2\text{O})]^+$.

| MOs | Energy (eV) | % of composition | |
|---------|-------------|------------------|-----|
| | | Cu | L |
| LUMO+5 | -3.16 | 55 | 45 |
| LUMO+4 | -3.52 | 03 | 97 |
| LUMO+3 | -3.88 | 05 | 95 |
| LUMO+2 | -4.10 | 01 | 99 |
| LUMO+1 | -4.71 | 02 | 98 |
| LUMO | -5.38 | 01 | 99 |
| HOMO | -9.03 | 02 | 98 |
| HOMO-1 | -9.09 | 02 | 98 |
| HOMO-2 | -9.57 | 10 | 90 |
| HOMO-3 | -10.16 | 0 | 100 |
| HOMO-4 | -10.67 | 05 | 95 |
| HOMO-5 | -10.72 | 03 | 97 |
| HOMO-6 | -10.93 | 10 | 90 |
| HOMO-7 | -11.35 | 13 | 87 |
| HOMO-8 | -11.65 | 03 | 97 |
| HOMO-9 | -11.71 | 37 | 63 |
| HOMO-10 | -12.15 | 01 | 99 |

Table 5Energy and composition of selected molecular orbitals (β -spin) of $[\text{Cu}(\text{L}) (\text{H}_2\text{O})]^+$.

| MOs | Energy (eV) | % of composition | |
|---------|-------------|------------------|-----|
| | | Cu | L |
| LUMO+5 | −3.52 | 03 | 97 |
| LUMO+4 | −3.87 | 05 | 95 |
| LUMO+3 | −4.09 | 01 | 99 |
| LUMO+2 | −4.69 | 02 | 98 |
| LUMO+1 | −5.33 | 01 | 99 |
| LUMO | −6.71 | 47 | 53 |
| HOMO | −8.99 | 03 | 97 |
| HOMO-1 | −9.15 | 02 | 98 |
| HOMO-2 | −10.14 | 0 | 100 |
| HOMO-3 | −10.19 | 16 | 84 |
| HOMO-4 | −10.68 | 02 | 98 |
| HOMO-5 | −10.74 | 05 | 95 |
| HOMO-6 | −11.01 | 12 | 88 |
| HOMO-7 | −11.37 | 36 | 64 |
| HOMO-8 | −11.52 | 27 | 73 |
| HOMO-9 | −11.75 | 29 | 71 |
| HOMO-10 | −12.09 | 30 | 70 |

**Fig. 9.** UV-Vis spectra of HL (—) and $[\text{Cu}(\text{L}) (\text{H}_2\text{O})][\text{ClO}_4]$ (—) in acetonitrile (inset shows the expanded spectrum for the complex).

values, the coordination geometry around copper ion is intermediate between trigonal bipyramidal and square pyramidal geometries and is better described as distorted square based pyramidal (DSBP) [42–44] with one water molecule occupying the axial position. In the complex copper atom is displaced by 0.248 Å above the N_2SO coordination plane and towards the elongated apical oxygen atom [45].

The presence of aqua ligand in the metal coordination sphere leads to the formation of H-bonding interaction, between the coordinated water molecules and the counter perchlorate anions, which connects the complexes about a center of symmetry. Packing diagram of the complex shows $\pi \dots \pi$ interactions between aromatic rings to form 1D supramolecular network (Fig. 4). Hence,

there is a series of essentially parallel units whose relative disposition is ideal for aromatic $\pi \dots \pi$ stacking interactions, forming a 1D supramolecular continuum. The dimer repeats along c-axis and they are under face-to-face $\pi \dots \pi$ interaction of pyridyl and aminothiophenyl ring to form the π -stack, with centroid–centroid distance of 3.549 (4) Å for $[\text{Cg}(4) \dots \text{Cg}(5)]$ (symmetry: x, 3/2-y, 1/2 + z) and 3.548 (4) Å $[\text{Cg}(5) \dots \text{Cg}(4)]$ (symmetry: x, 3/2-y, -1/2 + z) (where, $\text{Cg}(4) = \text{N1,C1,C2,C3,C4}$ and C5 and $\text{Cg}(5) = \text{C7,C8,C9,C10,C11}$ and C12).

3.3. DFT computation and electronic structure of $[\text{Cu}(\text{L}) (\text{H}_2\text{O})]^+$

To understand the electronic structure of the complex DFT calculation has been performed on $[\text{Cu}(\text{L}) (\text{H}_2\text{O})]^+$. The full geometry optimization for the compound has been carried out in the DFT/UB3LYP level. Some selected optimized bond parameters are given in Table 3. The optimized bond lengths and bond angles well reproduced the X-ray data of the complex. Optimized structure of $[\text{Cu}(\text{L}) (\text{H}_2\text{O})]^+$ is shown in Fig. 5. Contour plots of some selected molecular orbitals of α -spin and β -spin are shown in Figs. 6 and 7 respectively. Fig. 8 represents the spin density of the unpaired spin distributed over the coordinated atom along with major contribution on copper center. Energy and compositions of some selected molecular orbitals α -spin and β -spin are given in Tables 4 and 5 respectively.

3.4. TDDFT calculation and electronic transitions of $[\text{Cu}(\text{L}) (\text{H}_2\text{O})]^+$

The experimental electronic spectra of the compounds in acetonitrile are shown in Fig. 9. In 200–900 nm range the complex exhibits two very low intense peaks at 589 and 547 nm. Moderately intense sharp bands at 416 nm and 263 nm have been observed along with shoulders at 290 and 381 nm. To simulate the experimental electronic spectra of the complexes TDDFT calculations have been performed in acetonitrile. The weak bands at 589 and 547 nm correspond to $d-d$ transitions in the complex (Table 6). The strong peak at 416 nm has $\pi(\text{L}) \rightarrow \pi^*(\text{L})$ (intra-ligand charge transfer transition, ILCT) character. In addition, the broad peaks at 290 and 381 nm have mixed LMCT and ILCT character.

4. Conclusion

We have successfully synthesized thioether containing NSNO donor azo ligand (HL) showing hydrazoketo and azoenol tautomerism. The equilibrium between the hydrazoketo and azoenol forms of the ligand has been theoretically established. In the uncoordinated state the hydrazoketo form is predominating over azoenol form. In copper(II) complex the ligand is present as azoenol state. The electronic spectra and electronic structure of the complex has been extensively studied. The structures of the ligand and copper(II) complex have been established from single crystal X-ray studies. The complex forms 1-D supramolecular structure by H-bonding interactions and $\pi \dots \pi$ stacking of the aromatic rings.

Table 6Vertical electronic transitions of $[\text{Cu}(\text{L}) (\text{H}_2\text{O})]^+$ calculated by TDDFT/CPCM method.

| Excitation energy (eV) | Wavelength (nm) | Osc. strength (f) | Transition | Character |
|------------------------|-----------------|-------------------|--|--|
| 2.0155 | 615.2 | 0.0184 | (55%)HOMO-8(β) → LUMO(β) | $\text{Cu}(\text{d}\pi) \rightarrow \text{Cu}(\text{d}\pi)$ |
| 2.2646 | 547.5 | 0.0147 | (49%)HOMO-12(β) → LUMO(β) | $\text{Cu}(\text{d}\pi) \rightarrow \text{Cu}(\text{d}\pi)$ |
| 3.0626 | 404.8 | 0.0370 | (49%)HOMO-1(β) → LUMO+1(β) | $\text{L}(\pi) \rightarrow \text{L}(\pi^*)$ |
| 3.1621 | 392.1 | 0.0587 | (28%)HOMO-3(β) → LUMO(β) | $\text{L}(\pi) \rightarrow \text{L}(\pi^*)/\text{Cu}(\text{d}\pi)$ |
| 3.2061 | 386.7 | 0.0945 | (26%)HOMO-4(β) → LUMO(β) | $\text{L}(\pi) \rightarrow \text{L}(\pi^*)/\text{Cu}(\text{d}\pi)$ |
| 3.7143 | 333.8 | 0.4570 | (34%)HOMO-6(β) → LUMO(β) | $\text{L}(\pi) \rightarrow \text{L}(\pi^*)/\text{Cu}(\text{d}\pi)$ |
| 4.1254 | 300.5 | 0.0378 | (33%)HOMO-2(β) → LUMO+1(β) | $\text{L}(\pi) \rightarrow \text{L}(\pi^*)$ |

Acknowledgment

Financial support received from the Department of Science and Technology, New Delhi, India (No. SB/EMEQ–242/2013) is gratefully acknowledged. A. K. Pramanik and D. Sarkar acknowledge CSIR, New Delhi, India for fellowship.

Appendix A. Supplementary data

Supplementary data related to this article can be found at <http://dx.doi.org/10.1016/j.molstruc.2015.06.048>.

References

- [1] J. Koh, A.J. Greaves, *Dyes Pigments* 50 (2001) 117–126.
- [2] N. Sekar, *Colourage* 46 (1999) 63–65.
- [3] H.E. Katz, K.D. Singer, J.E. Sohn, C.W. Dirk, L.A. King, H.M. Gordon, *J. Am. Chem. Soc.* 109 (1987) 6561–6563.
- [4] S. Wang, S. Shen, H. Xu, *Dyes Pigments* 44 (2000) 195–198.
- [5] K. Maho, T. Shintaro, K. Yutaka, W. Kazuo, N. Toshiyuki, T. Mosahiko, *Jpn. J. Appl. Phys.* 42 (2003) 1068–1075.
- [6] G. Hallas, J.H. Choi, *Dyes Pigments* 40 (1999) 119–129.
- [7] P. Gregory, D.R. Waring, G. Hallos, *The Chemistry and Application of Dyes*, Plenum Press, London, 1990, pp. 18–20.
- [8] S. Wu, W. Qian, Z. Xia, Y. Zou, S. Wang, S. Shen, *Chem. Phys. Lett.* 330 (2000) 535–540.
- [9] P. Gilli, V. Bertolasi, L. Pretto, A. Lycka, G. Gilli, *J. Am. Chem. Soc.* 124 (2002) 13554–13567.
- [10] R.C. Cox, E. Buncel, in: S. Patai (Ed.), *The Chemistry of the Hydrazo, Azo and Azoxy Groups*, Wiley, Chichester, 1970, p. 838.
- [11] J.A. Connor, R.J. Kennedy, M.H. Dawes, M.B. Hursthouse, N.P.C. Walker, *J. Chem. Soc. Perkin Trans. 2* (1990) 203–207.
- [12] A.C. Olivieri, R.B. Wilson, I.C. Paul, D.Y. Curtin, *J. Am. Chem. Soc.* 111 (1989) 5525–5532.
- [13] G. Gilli, F. Belucci, V. Ferretti, V. Bertolasi, *J. Am. Chem. Soc.* 111 (1989) 1023–1028.
- [14] V. Bertolasi, P. Gilli, V. Ferretti, G. Gilli, *J. Am. Chem. Soc.* 113 (1991) 4917–4925.
- [15] G. Gilli, V. Bertolasi, V. Ferretti, P. Gilli, *Acta Crystallogr. Sect. B* 49 (1993) 564–576.
- [16] V. Bertolasi, P. Gilli, V. Ferretti, G. Gilli, *Chem. Eur. J.* 2 (1996) 925–934.
- [17] V. Bertolasi, V. Ferretti, G. Gilli, Y.M. Issa, O.E. Sherif, *J. Chem. Soc. Perkin Trans. 2* (1993) 2223–2228.
- [18] V. Bertolasi, L. Nanni, P. Gilli, V. Ferretti, G. Gilli, Y.M. Issa, O.E. Sherif, *New. J. Chem.* 18 (1994), 251–161.
- [19] V. Bertolasi, L. Pretto, G. Gilli, P. Gilli, *Acta Crystallogr. Sect. B* 62 (2006) 850–863.
- [20] P. Chattopadhyay, Y.H. Chiu, J.M. Lo, C.S. Chung, T.H. Lu, *Appl. Radiat. Isot.* 52 (2000) 217.
- [21] W.C. Wolsey, *J. Chem. Educ.* 50 (1973) A335.
- [22] L.J. Farrugia, *J. Appl. Cryst.* 45 (2012) 849.
- [23] G.M. Sheldrick, *Acta Crystallogr. Sect. A* 64 (2008) 112.
- [24] SAINT Plus, Data Reduction and Correction Program, v. 6.01, Bruker AXS, Madison, Wisconsin, USA, 1998.
- [25] Bruker APEX2, SAINT and SADABS, Bruker AXS Inc, Madison, Wisconsin, USA, 2010.
- [26] L.J. Farrugia, ORTEP-3 for windows, *J. Appl. Cryst.* 30 (1997) 565.
- [27] M.J. Frisch, G.W. Trucks, H.B. Schlegel, G.E. Scuseria, M.A. Robb, J.R. Cheeseman, G. Scalmani, V. Barone, B. Mennucci, G.A. Petersson, H. Nakatsuji, M. Caricato, X. Li, H.P. Hratchian, A.F. Izmaylov, J. Bloino, G. Zheng, J.L. Sonnenberg, M. Hada, M. Ehara, K. Toyota, R. Fukuda, J. Hasegawa, M. Ishida, T. Nakajima, Y. Honda, O. Kitao, H. Nakai, T. Vreven, J.A. Montgomery Jr., J.E. Peralta, F. Ogliaro, M. Bearpark, J.J. Heyd, E. Brothers, K.N. Kudin, V.N. Staroverov, R. Kobayashi, J. Normand, K. Raghavachari, A. Rendell, J.C. Burant, S.S. Iyengar, J. Tomasi, M. Cossi, N. Rega, J.M. Millam, M. Klene, J.E. Knox, J.B. Cross, V. Bakken, C. Adamo, J. Jaramillo, R. Gomperts, R.E. Stratmann, O. Yazyev, A.J. Austin, R. Cammi, C. Pomelli, J.W. Ochterski, R.L. Martin, K. Morokuma, V.G. Zakrzewski, G.A. Voth, P. Salvador, J.J. Dannenberg, S. Dapprich, A.D. Daniels, Ö. Farkas, J.B. Foresman, J.V. Ortiz, J. Cioslowski, D.J. Fox, Gaussian 09, Revision D.01, Gaussian, Inc., Wallingford CT, 2009.
- [28] A.D. Becke, *J. Chem. Phys.* 98 (1993) 5648–5652.
- [29] C. Lee, W. Yang, R.G. Parr, *Phys. Rev. B* 37 (1988) 785–789.
- [30] P.J. Hay, W.R. Wadt, *J. Chem. Phys.* 82 (1985) 270–283.
- [31] W.R. Wadt, P.J. Hay, *J. Chem. Phys.* 82 (1985) 284–298.
- [32] P.J. Hay, W.R. Wadt, *J. Chem. Phys.* 82 (1985) 299–310.
- [33] R. Bauernschmitt, R. Ahlrichs, *Chem. Phys. Lett.* 256 (1996) 454–464.
- [34] R.E. Stratmann, G.E. Scuseria, M.J. Frisch, *J. Chem. Phys.* 109 (1998) 8218–8224.
- [35] M.E. Casida, C. Jamorski, K.C. Casida, D.R. Salahub, *J. Chem. Phys.* 108 (1998) 4439–4449.
- [36] V. Barone, M. Cossi, *J. Phys. Chem. A* 102 (1998) 1995–2001.
- [37] M. Cossi, V. Barone, *J. Chem. Phys.* 115 (2001) 4708–4717.
- [38] M. Cossi, N. Rega, G. Scalmani, V. Barone, *J. Comput. Chem.* 24 (2003) 669–681.
- [39] N.M. O'Boyle, A.L. Tenderholt, K.M. Langner, *J. Comput. Chem.* 29 (2008) 839–845.
- [40] S. Sarkar, A. Patra, M.G.B. Drew, E. Zangrandi, P. Chattopadhyay, *Polyhedron* 28 (2009) 1.
- [41] A.W. Addison, T.N. Rao, J. Reedijk, J. van Rijn, G.C. Verschoor, *J. Chem. Soc. Dalton Trans.* (1984) 1349–1356.
- [42] G. Murphy, P. Nagle, B. Murphy, B. Hathaway, *J. Chem. Soc. Dalton Trans.* (1997) 2645–2652.
- [43] G. Murphy, C. Murphy, B. Murphy, B. Hathaway, *J. Chem. Soc. Dalton Trans.* (1997) 2653–2660.
- [44] G. Murphy, C. O'Sullivan, B. Murphy, B. Hathaway, *Inorg. Chem.* 37 (1998) 240–248.
- [45] D.-M. Feng, H.-Y. He, H.-X. Jin, L.-G. Zhu, Z. Kristallogr., *New. Cryst. Struct.* 220 (2005) 429–430.